Author's Accepted Manuscript

www.elsevier.com/locate/talanta

The synthesis of a smart streptavidin-functionalized poly(N-isopropylacrylamide) composite and its application in the separation and detection of virus nucleic acid

Xinxin Wang, Mingyuan Du, Guobin Mao, Jiao Zheng, Jinyang Chen, Xinghu Ji, Zhike He

PII: S0039-9140(17)31268-7
DOI: https://doi.org/10.1016/j.talanta.2017.12.068
Reference: TAL18204

To appear in: *Talanta*

Received date: 9 September 2017
Revised date: 13 December 2017
Accepted date: 21 December 2017

Cite this article as: Xinxin Wang, Mingyuan Du, Guobin Mao, Jiao Zheng, Jinyang Chen, Xinghu Ji and Zhike He, The synthesis of a smart streptavidin-functionalized poly(N-isopropylacrylamide) composite and its application in the separation and detection of virus nucleic acid, *Talanta,* https://doi.org/10.1016/j.talanta.2017.12.068

The synthesis of a smart streptavidin-functionalized poly(N-isopropylacrylamide) composite and its application in the separation and detection of virus nucleic acid

Xinxin Wang, Mingyuan Du, Guobin Mao, Jiao Zheng, Jinyang Chen, Xinghu Ji, Zhike He*

Key Laboratory of Analytical Chemistry for Biology and Medicine (Ministry of Education), College of Chemistry and Molecular Sciences, Wuhan University, Wuhan 430072, China

ABSTRACT

A new kind of polymeric material (PNIPAAm-co-SA) was prepared by conjugating a thermosensitive polymer, Poly (N-isopropylacrylamide) (PNIPAAm) with streptavidin (SA). This smart prepared composite displayed a controllable conformation change between an expanded and a collapsed form, below or above its lower critical solution temperature (LCST). Differential scanning calorimetry (DSC) analysis demonstrated that the PNIPAAm-co-SA bioconjugate showed the same LCST as the original synthetic polymer, PNIPAAm, which was also 32 °C. Based on the specific interaction between SA and biotin, a higher capture efficiency of PNIPAAm-co-SA, which was almost 100% in PBS buffer solution and above 70% in serum was obtained, respectively. And the high affinity between PNIPAAm-co-SA

and biotin was still maintained after three heating cycles. Subsequently, the variola virus (small pox, VV) oligonucleotide sequence was chosen as a model to demonstrate the sensitivity of the biosensor which was fabricated based on PNIPAAm-co-SA. The biosensor exhibited the ability to separate and enrich targets from complicated system with its phase transition ability, and high sensitivity toward VV-targets were achieved. Moreover, other types of targets such as proteins and cells, could be detected by changing the biotin-captures, which indicated the broad applicability of biosensors based on this smart polymer material.

KEYWORDS: thermosensitive polymer; streptavidin; separation; detection; nucleic acid

1. INTRODUCTION

Thermosensitive polymers are soluble in a solvent (water) at low temperatures but become insoluble when the temperature rises above a certain temperature threshold defined as lower critical solution temperature (LCST) [1-4]. The uniqueness of these polymers lies not only on the fast macroscopic changes occurring in their structure but also the reversibility of these transitions [5]. Poly (N-isopropylacrylamide) (PNIPAAm), a kind of thermosensitive polymer, gained its popularity mainly because of the sharpness of its phase transition. The LCST of PNIPAAm is about 32 °C, which is close to the physiological temperature and resulting in the wide applications in biomaterial field [6-8]. At temperatures above the LCST, the PNIPAAm chains are dehydrated, forming compact structures that can

aggregate and precipitate from solution. It could be physically mixed with or chemically conjugated to biomolecules to yield a large family of polymer-biomolecule systems which can respond to biological, physical and chemical stimuli [9,10]. Proteins modified with PNIPAAm are also known to precipitate in aqueous solution at temperatures above the LCST [11]. It was reported that a thermodynamic controlled strategy was proposed for realizing in situ conformational transition of polymer-peptide conjugates at cell surfaces to monitor HER2 receptor clustering, which finally result in effective inhibition of the breast cancer cell proliferation [12]. John M. Hoffman et al. utilized stimuli-responsive polymer-antibody conjugates in microfluidic immunoassay to enable rapid biomarker purification and enrichment as well as sensitive detection [13]. However, there was a problem that once the target changed, it was necessary to establish a new conjugation having the specific combination with the target.

SA, a kind of homotetramer [14], can tightly bind to a small molecule, biotin [15], which is widely applied in many research fields [16-18]. Up to four biotin can be tightly bound to streptavidin simultaneously with an affinity constant of 2.5×10^{13} L mol^{-1}, which is the strongest non-covalent interaction among those reported interactions between two biomolecules [14,19]. Herein, to solve the above mentioned problem of application limitation, we proposed a novel strategy to conjugate the thermosensitive polymer, PNIPAAm, with the protein, streptavidin (SA) to yield the desired material, PNIPAAm-co-SA. The advantages of PNIPAAm-co-SA are as follows. Firstly, the specific interaction between SA and biotin is widely utilized in

many applications, which provides the high universality of this material. Secondly, the preparation of this material is simple, without multiple synthesis process and complex purification. Thirdly, compared with heterogeneous system such as magnetic beads [20,21], the polymer chains of PNIPAAm hydrate to form expanded structures in water at temperatures below its LCST [22], resulting in a homogeneous system [23], which can make reaction more fully. Finally, this material is easy to precipitate in aqueous solution at temperatures above the LCST, which can allow us to enrich and separate the target compounds from samples, reducing the background and improving the sensitivity [24].

It is known that the detections of biomolecules have become more and more significant in early diagnostic tests for mutation, early cancer detection and treatment of diseases [25-27]. A specific sequence DNA detection can help us to deal with clinical diagnosis, biomedical studies, gene expression analysis, pathology and molecular biology research [28-30]. However, the low concentrations of diseases-related DNA biomarkers in biological samples and the numerous interferences in complex system make it highly desirable to develop sensitive and universal methods for DNA detection [31-33]. Various DNA biosensors have been established based on the strategies such as fluorescence [34-36], electrochemical luminescence [37，38], surface plasma resonance spectroscopy [39] and so on.

To verify the utilization potentiality of PNIPAAm-co-SA, the variola virus (small pox, VV) oligonucleotide sequence [31] was chosen as a DNA model to demonstrate the superiority of the biosensor fabricated with this material and biotin functionalized

DNA (Biotin-VV). Firstly, PNIPAAm-co-SA and Biotin-VV formed complexes by interaction of SA and biotin. Next, targets can be captured by the Biotin-VV in the bases of complementary matching principle. Later, in order to produce fluorescence signals, ROX functionalized DNA (VV-ROX) was utilized to react with the other part of the targets. At last, with the superior thermosensitive characteristic of PNIPAAm-co-SA, the detection was achieved. The experimental results showed that the biosensor exhibited high sensitivity and selectivity for target DNA detection. Moreover, this material can be expanded for the detection of the other DNA targets just by changing the sequence of the functionalized DNA probe. And other proteins also could be detected by introducing the corresponding biotin functionalized aptamers or biotin conjugated antibodies [40,41].

2. EXPERIMENTAL SECTION

2.1. Materials and reagents

N-isopropylacrylamide (NIP), acrylic acid N-hydroxysuccinimide ester (NAS), ammonium persulfate (APS), N,N,N,N-tetramethylethylenediamine (TEMED), trihydroxymethy laminomethane (Tris), sodium phosphate dibasic, sodium phosphate monobasic dihydrate, potassium chloride, magnesium chloride, sodium chloride, were obtained from Sigma-Aldrich (USA). SA was purchased from Amresco (USA). All above reagents are of analytical-reagent grade or better. Hydrochloric acid was purchased from Sinopharm Chemical Reagent Co., Ltd. All oligonucleotides with different sequences were synthesized and high-performance

liquid chromatography (HPLC) purified by Sangon Biotechnology Co. Ltd. (Shanghai, China). The sequences of the oligonucleotides are as follows:

BF-DNA: 5'-biotin-AAA AAA AAA AAA AAA AAA-6-FAM-3'

F-DNA: 5'-AAA AAA AAA AAA AAA AAA-6-FAM-3'

Biotin-VV: 5'-biotin-TTT AAA CTG ATT ACT ATT GCA-3'

VV-ROX: 5' -TCT TCC GTT ACA ACT AAA TTT-ROX-3'

VV-target: 5' -AGT TGT AAC GGA AGA TGC AAT AGT AAT CAG-3'

MT2: 5' -AGT TGT AAC GGA ATC TGC AAT AGT AAT CAG -3'

MT3: 5' -AGT TGT AAC GGA TTC TGC AAT AGT AAT CAG -3'

MT4: 5' -AGT TGT AAC GGC TTC TGC AAT AGT AAT CAG -3'

MT5: 5' -AGT TGT AAC GCC TTC TGC AAT AGT AAT CAG -3'

Ultrapure water was produced by a Milli-Q Academic purification set (Millipore, USA). PNIPAAm-co-SA was characterized by FT-IR (NICOLET 5700 FTIR Spectrometer, Thermo Electron Corporation, USA) and DSC （Q200， TA Instruments， USA）. The purification process was monitored and recorded using a UV-2250 spectrophotometer (Shimadzu, Japan) using a 1-cm path length quartz cuvette. Fluorimetric spectra were obtained with a RF-5301PC spectrophotometer (Shimadzu, Japan) equipped with a 150 W xenon lamp (Ushio Inc, Japan).

2.2. Preparation of PNIPAAm-co-SA

As shown in Figure 1, PNIPAAm-co-SA was constructed using a coupling reagent NAS which can react with SA via amide linkage function and polymerize with NIP.

Briefly, 100 μL of 2 mg mL^{-1} SA was coupled with 250 μL NAS in DMSO of 1 mg mL^{-1}, and incubated at 37 °C under stirring for 1 h. Afterwards, 60 mg NIP, 10 mg APS and 10 μL TEMED were added into the coupling product in 5 mL of PBS buffer solution 1 (Na_2HPO_4 10 mM, NaH_2PO_4 10 mM, NaCl 15 mM, pH 7.4). After polymerization for 2 h by continuous shaking at 25 °C, PNIPAAm-co-SA was precipitated at 37 °C for 5 min and separated from unreacted monomers, SA and small molecule impurities by centrifugation for 5 min at 37 °C (8000 rpm) and then resolved in 5 mL of cold PBS buffer solution 1. The purification cycle was repeated for 3 times. Later, PNIPAAm-co-SA was resuspended in 5 mL of PBS buffer solution 1 and stored at 4 °C before use.

2.3. SA linkage rate of PNIPAAm-co-SA

Up to four biotin can be tightly bound to SA simultaneously, DNA modified with biotin and 6-FAM (BF-DNA) was utilized for the calculation of SA linkage rate. Concentration of 12 nM, 20 nM, 40 nM, 100 nM, 200 nM, 400 nM DNA were reacted with 50 μL PNIPAAm-co-SA at 25 °C for 30 min to form fluorescent compounds which can indicate the amount of SA connected in PNIPAAm-co-SA. Therewith, the compounds was precipitated at 37 °C for 5 min and centrifuged for 3 min at 37 °C (13000 rpm) and then resolved in 500 μL of cold PBS buffer solution 2 (Na_2HPO_4 10 mM, NaH_2PO_4 10 mM, NaCl 150 mM, pH 7.4), and repeated for 3 times. Fluorescence detection proceeded after overall steps.

2.4. Capture capability of PNIPAAm-co-SA in buffer solution and serum

PNIPAAm-co-SA was thought to have an excellent capture capability for biotin modified targets. Therefore, BF-DNA was introduced to investigate its capture capability in buffer solution and serum, respectively. Firstly, different concentrations of BF-DNA and 50 μL PNIPAAm-co-SA were added into 500 μL PBS buffer solution 2 and serum, respectively, and then the mixtures were shaking at 25 °C for 30 min to form SA-biotin structures. After precipitating and centrifuging the complexes three times, they were added into 500 μL cold buffer solution 2. Meanwhile, in order to explore the influence of nonspecific adsorption, only 6-FAM modified DNA(F-DNA) was investigated in the same way. The fluorescence signal of each product was individually analyzed and the intensity was recorded.

2.5. Storage life test

50 μL newly synthesized and stored for 45 days PNIPAAm-co-SA were mixed with 6 nM BF-DNA to investigate the time stability of this material, respectively. The products was precipitated and centrifuged uniformly. The analyses were performed using a fluorescence spectrophotometer.

2.6. Procedure for DNA detection

For the detection of the variola virus (small pox, VV) oligonucleotide sequence, VV-targets were stored in PBS buffer solution 2, then diluted to 1.00×10^{-7} M. 60 μL PNIPAAm-co-SA was mixed with 40 μL of 1.00×10^{-6} M Biotin-VV, different

concentrations of VV-targets and 40 μL of 1.00×10^{-6} M VV-ROX in 500 μL PBS buffer solution 2 and incubated for 2 h. Finally, the solution obtained from the hybridization reaction was precipitated and centrifuged three times, and redissolved in 300 μL cold PBS buffer solution 2 for fluorescence detection. For the detection of VV-targets in human serum, the volume ratio of human serum in the final VV-targets solution was fixed at 20%, and the other procedures were the same as the detection in the PBS buffer solution 2.

3. RESULTS AND DISCUSSION

3.1. Preparation and characterization of PNIPAAm-co-SA

Thermosensitive material PNIPAAm-co-SA was prepared via coupling reagent NAS which can form amide bonds with amino groups on SA, and occur polymerization reaction with NIP. The FT-IR spectra of PNIPAAm-co-SA were analyzed at room temperature in the region of 4000 and 500 cm^{-1}, with a resolution of 2 cm^{-1} and 20 scans. As shown in Figure 2A, the spectra showed the typical amide I band (1646.94 cm^{-1}) consisting of C=O stretch of PNIPAAm, and an amide II band (1544.73 cm^{-1}), including N-H vibration. These bands were characteristic peaks of PNIPAAm. The peaks at 3286.16 cm^{-1} and 3436.58 cm^{-1} were assigned to the N-H stretching vibration. The peak in range between 3000 and 2835 cm^{-1} belongs to the C-H stretching vibration, in which the peaks at 2971.81 cm^{-1} and 2873.46 cm^{-1} were assigned to asymmetric and symmetric vibrations of methyl group, and the peak at 2931.32 cm^{-1} was due to the asymmetric vibration of methylene group. The peak at

1457.54 cm^{-1} belongs to the asymmetric bending vibration of methylene group. Furthermore, the peak ranging from 1400-1355 cm^{-1} corresponded to the bending vibrations of isopropyl groups. PNIPAAm characteristic peaks in the FT-IR spectra of PNIPAAm-co-SA synthesized were consistent with those in the FT-IR spectra of PNIPAAm reported previously [42,43]. It suggested that PNIPAAm-co-SA synthesized utilizing this method indeed consisted the functional group of PNIPAAm, which ensured the thermosensitive characteristic of this material.

Differential scanning calorimetry (DSC) was used to measure the lower critical solution temperature (LCST) of PNIPAAm-co-SA. Then DSC thermogram was measured by a central processor from 10 to 40 °C. The heating rate was controlled at 1 °C min^{-1}. As shown in Figure 2B, there was an obvious endothermic peak at 32 °C, which was in accordance with the theoretical value of PNIPAAm [44]. We suspected that it was due to the strong hydrophobic interaction between the polymer rather than hydrophilic interaction between water molecules, resulting in precipitation and phase separation of polymer, which was caused by an endothermic process, ultimately producing the endothermic peak in the DSC thermogram. It indicated that the temperature sensitive property of PNIPAAm related groups in PNIPAAm-co-SA was not been influenced by the addition of SA. Furthermore, the LCST of PNIPAAm-co-SA was also 32 °C, which was close to the physiological temperature, availing for the separation, enrichment and detection of biological samples.

In order to verify that the SA was attached to instead of inclusion in the polymer, PNIPAAm-co-SA was characterized by UV−vis. After conjugation, the solution was

processed with thermal precipitation to separate unreacted monomers, SA and small molecule impurities in the solution by pelleting PNIPAAm-co-SA. Then UV−vis spectrum of the resuspended pellet (Figure 2C, red) exhibited a peak absorbance around 280 nm, which confirmed SA was conjugated. Instead, the supernatant (Figure 2C, blue) and PNIPAAm (Figure 2C, black), exhibited no absorption peak. Therefore, the UV−vis spectrum indicated that SA bonds to PNIPAAm through chemical reaction rather than physical absorption.

A set of control experiments were carried out to demonstrate that PNIPAAm-co-SA has the ability of specific binding with biotin. In theory, four biotin can be tightly bound to streptavidin at the same time. In the case of the simultaneous existence of SA and biotin, A strong fluorescence signal was detected (Figure 2D a). On the contrary, as shown in Figure 2D b , c , d, there are almost no fluorescence signal. The results indicate that the fluorescence signal is produced by the specific binding of SA and biotin, rather than the nonspecific adsorption of 6-FAM labeled DNA on the surface of PNIPAAm-co-SA .

3.2. Linkage rate of SA

In theory, four biotin can be tightly bound to SA simultaneously. When the fluorescence intensity of BF-DNA in the fluorescent compounds no longer increased with the amount added, the combination of SA and biotin reached saturation. The concentration of BF-DNA corresponding to this fluorescence intensity can be used to calculate the concentration of SA in the material. The fluorescence intensities of the

compounds for various BF-DNA concentrations were shown in Figure 3. Initially the fluorescence intensity increased with increasing concentration of BF-DNA. Nevertheless, when the concentration of BF-DNA increased to a certain degree, 200 nM, which was close to the maximum amount SA can combine with, the fluorescence intensity reached to a platform value. The amount of SA added in the synthesis process was 60 nM.

The calculation result of SA linkage rate is as follows:

$$\frac{2.00\times10^{-7}}{4.0\times6.0\times10^{-8}}=83\%$$

As four binding sites of SA could not be fully saturated in the actual experiment, SA linkage rate was greater than or equal to 83%.

3.3. Capture capability of PNIPAAm-co-SA in buffer solution and serum

A strong specific binding interaction between SA and biotin ensures that PNIPAAm-co-SA can capture BF-DNA efficiently. As shown in Figure 4, the standard curve was plotted at BF-DNA concentrations range (0.50 – 7.00 nM). In PBS buffer solution, almost all of the BF-DNA can be separated from the solution, which indicated that PNIPAAm-co-SA has an excellent ability to capture the targets modified with biotin. Likewise, the capture rate of PNIPAAm-co-SA in serum was also explored. However, due to the complexity of the matrix of serum, the capture efficiency is relatively lower than that in buffer solution. The calculated capture capability of PNIPAAm-co-SA in buffer solution and serum are summarized in Table 1.

In order to investigate the nonspecific adsorption, F-DNA was utilized as a control to perform the same experiments in buffer solution and serum, respectively. As shown in Figure 5, there is really a sharp contrast between the fluorescence intensity produced by BF-DNA and F-DNA. Almost no fluorescence signal was detected in the absence of biotin, proving that nonspecific adsorption was very low in the test.

3.4. Investigation of storage life

The storage life of materials is of vital importance for its applications. Long storage life ensures high stability. High stability ensures high efficiency of separation and enrichment, high accuracy of detection, as well as low cost. The storage life analysis was investigated by using two kinds of PNIPAAm-co-SA which was newly-synthesized and stored for 45 days at 4 ℃, respectively. As shown in Figure 6, the fluorescence intensity almost don't decreased even though the compound was stored for 45 days, indicating that PNIPAAm-co-SA still had a strong binding capacity for the targets which modified with biotin. The good time stability of this material is beneficial to its applications.

3.5. DNA detection

Firstly, we investigated the application of the PNIPAAm-co-SA in the detection of single-stranded DNA (ssDNA). The DNA detection is based on enrichment with PNIPAAm-co-SA and the strict complementary nature of the base pairs. In addition, PNIPAAm-co-SA as the captor can separate the targets from the complex

environments to reduce the background, thus improving the detection sensitivity. Figure 7A illustrates the process of the detection. Hence, under the optimal condition, we investigated the sensitivity of the strategy by utilizing the oligonucleotide sequence associated with variola virus (small pox, VV) as the target model. As described in Figure 7B, the fluorescence intensity increases gradually with the increase of the concentration of VV-targets, and the fluorescence intensity shows a clear linear dependence on the VV-targets concentration over the range from 0.50 to 20.00 nM, and the regression equation is y=30.6x+16.0 (R^2 = 0.99633). The limit of detection (LOD) for VV-targets is calculated to be 57 pM according to the equation C_{LOD}=3S/k, where C_{LOD} is the limit of detection, S is standard deviation of the blank (N = 10), and k is the slope of regression equation. Therefore, the proposed method possesses a desired sensitivity for DNA detection.

The selectivity of this method was tested by measuring and comparing the responses of target DNA with two-base mismatched target DNA (MT2), three-base mismatched target DNA (MT3), four-base mismatched target DNA (MT4) and five-base mismatched target DNA (MT5), respectively. As shown in Figure 8, the same concentration of mismatched target yielded a significantly lower fluorescence signal compared to that of target DNA. These results revealed that this proposed method exhibited a good selectivity to detect target DNA.

In order to investigate the interference of impurity in human serum, the method has been employed to analyze VV-targets in human serum. The buffer solution was introduced to mix with human serum for helping with DNA hybridization. According

to the results summarized in Table 2, the fluorescence intensities detected in the diluted human serum (20%) had slightly differences with those obtained in buffer solution. The recoveries of VV-targets in human serum samples are within the acceptable range, and the standard deviation of each found is relatively smaller. Therefore, it is proved that PNIPAAm-co-SA could quantify the DNA concentration in complex biological samples.

4. CONCLUSION

In conclusion, an universal protein modified thermosensitive polymer, PNIPAAm-co-SA conjugation was prepared. This conjugation exhibits a rapid response to temperature change and significant phase separation above the LCST. Homogeneous system is advantageous to the full and quick reaction of the reactants. And heterogeneous system can be favor to the separation of the targets from complex environments, reducing the background. The phase change capability between homogeneous and heterogeneous phases of PNIPAAm-co-SA promotes it to have a good application potential in the fields of separation, enrichment and detection of biological samples. Given this, PNIPAAm-co-SA was utilized to develop a highly sensitive DNA detection biosensor by introducing biotin-modified DNA sequence as capture DNA into this system. In addition, this method can be expanded to detect a wide range of samples with a rational design of the corresponding captures. In view of these advantages, PNIPAAm-co-SA has great potential in the area of biological applications

ACKNOWLEDGEMENTS

This work was supported by the National Natural Science Foundation of China (21475101, 21675119).

Conflicts of interest: none

REFERENCE

[1] S. T. Jones, Z. Walsh-Korb, S. J. Barrow, S. L. Henderson, J. del Barrio, O. A. Scherman, The importance of excess Poly (N-isopropylacrylamide) for the aggregation of Poly (N-isopropylacrylamide)-coated gold nanoparticles, ACS nano 10 (3) (2016**)** 3158-3165.

[2] S. Kwan, M. Marić, Thermoresponsive polymers with tunable cloud point temperatures grafted from chitosan via nitroxide mediated polymerization, Polymer 86 (2016) 69-82.

[3] R. Iwai, S. Kusakabe, Y. Nemoto, Y. Nakayama, Deposition gene transfection using bioconjugates of DNA and thermoresponsive cationic homopolymer, Bioconjugate Chem. 23 (4) (2012) 751-757.

[4] A. Kumar, A. Srivastava, I. Y. Galaev, B. Mattiasson, Smart polymers: physical forms and bioengineering applications, Prog. Polym. Sci. 32 (10) (2007) 1205-1237.

[5] W. Hong, S. Lee, E. Jae Kim, M. Lee, Y. Cho, A reusable electrochemical immunosensor fabricated using a temperature-responsive polymer for cancer

bomarker proteins, Biosens. Bioelectron. 78 (2016) 181-186.

[6] T. Kawano, Y. Niidome, T. Mori, Y. Katayama, T. Niidome, PNIPAM gel-coated gold nanorods for targeted delivery responding to a near-infrared laser, Bioconjugate Chem. 20 (2009) 209–212.

[7] J. R. Francica, G. M. Lynn, R. Laga, M. G. Joyce, T. J. Ruckwardt, K. M. Morabito, M. Chen, R. Chaudhuri, B. Zhang, M. Sastry, A. Druz, K. Ko, M. Choe, M. Pechar, I. S. Georgiev, L. A. Kueltzo, L. W. Seymour, J. R. Mascola, P. D. Kwong, B. S. Graham, R. A. Seder, Thermoresponsive polymer nanoparticles co-deliver RSV F trimers with a TLR-7/8 adjuvant, Bioconjugate Chem. 27 (10) (2016) 2372-2385.

[8] T. Liu, S. Liu, Responsive polymers-based dual fuorescent chemosensors for Zn^{2+} ions and temperatures working in purely aqueous media, Anal. Chem. 83 (7) (2011) 2775-2785.

[9] J. Miao, Z. Cao, Y. Zhou, C. Lau, J. Lu, Instantaneous derivatization technology for simultaneous and homogeneous determination of multiple DNA targets, Anal. Chem. 80 (2008) 1606-1613.

[10] S. Sugiura, W. Imano, T. Takagi, K. Sakai, T. Kanamori, Thermoresponsive protein adsorption of Poly (N-isopropylacrylamide)-modified streptavidin on polydimethylsiloxane microchannel surfaces, Biosens. Bioelectron. 24 (5) (2009) 1135-1140.

[11] D.Roy, B. J. Nehilla, J. J. Lai, P. S. Stayton, Stimuli-responsive polymer-antibody conjugates via RAFT and tetrafluorophenyl active ester chemistry, ACS Macro Lett. 2 (2) (2013) 132-136.

[12] S. L. Qiao, Y. Wang, Y. X. Lin, H. W. An, Y. Ma, L. L. Li, L. Wang, H. Wang, Thermo-controlled in situ phase transition of polymer-peptides on cell surfaces for high-performance proliferative inhibition, ACS Appl. Mater. Interfaces 8 (27) (2016) 17016-17022.

[13] J. M. Hoffman, P. S. Stayton, A. S. Hoffman, J. J.Lai, Stimuli-responsive reagent system for enabling microfluidic immunoassays with biomarker purification and enrichment, Bioconjugate Chem. 26 (1) (2015) 29-38.

[14] J. Ylikotila, L. Valimaa, H. Takalo, K. Pettersson, Improved surface stability and biotin binding properties of streptavidin coating on polystyrene, Colloids Surf. B 70 (2) (2009) 271-277.

[15] M. Fairhead, G. Veggiani, M. Lever, J. Yan, D. Mesner, C. V. Robinson, O. Dushek, P. A. van der Merwe, M. Howarth, SpyAvidin hubs enable precise and ultrastable orthogonal nanoassembly, J. Am. Chem. Soc. 136 (35) (2014) 12355-12363.

[16] M. Carlomagno, G. Lassabe, M. Rossotti, A. Gonzalez-Techera, L. Vanrell, G. Gonzalez-Sapienza, Recombinant sreptavidin nanopeptamer anti-immunocomplex assay for noncompetitive detection of small analytes, Anal. Chem. 86 (20) (2014) 10467-10473.

[17] Y. P. Ohayon, R. Sha, O. Flint, W. Liu, B. Chakraborty, H. K. K. Subramanian, J. Zheng, A. R. Chandrasekaran, H. O. Abdallah, X. Wang, X. Zhang, N. C. Seeman, Covalent linkage of one-dimensional DNA arrays bonded by paranemic cohesion, ACS nano 9 (10) (2015) 10304–10312.

[18] M. Boutard, L. Ettwiller, T. Cerisy, A. Alberti, K. Labadie, M. Salanoubat, I. Schildkraut, A. C. Tolonen, Global repositioning of transcription start sites in a plant-fermenting bacterium, Nat. Commun. 7 (2016) 13783.

[19] M. Zhang, S. Biswas, W. Deng, H. Yu, The crystal structure of monovalent streptavidin, Sci. Rep. 6 (2016) 35915.

[20] N. Li, J. Chen, M. Luo, C. Chen, X. Ji, Z. He, Highly sensitive chemiluminescence biosensor for protein detection based on the functionalized magnetic microparticles and the hybridization chain reaction, Biosens. Bioelectron, 87 (2017) 325-331.

[21] Y. Liu, M. Luo, J. Yan, X. Xiang,; X. Ji, G. Zhou, Z. He, An ultrasensitive biosensor for DNA detection based on hybridization chain reaction coupled with the efficient quenching of a ruthenium complex to CdTe quantum dots, Chem. Commun. 49 (67) (2013) 7424-7426.

[22] G. Zhao, W. Chen, Enhanced PVDF membrane performance via surface modification by functional polymer Poly(N-isopropylacrylamide) to control protein adsorption and bacterial adhesion, React. Funct. Polym. 97 (2015) 19-29.

[23] A. S. Hoffman, Stimuli-responsive polymers: biomedical applications and challenges for clinical translation, Adv. Drug. Deliv. Rev. 65 (1) (2013) 10-16.

[24] A. Barhoumi, W. Wang, D. Zurakowski, R. S. Langer, D. S. Kohane, Photothermally targeted thermosensitive polymer-masked nanoparticles, Nano Lett. 14 (7) (2014) 3697-3701.

[25] S. H. Qaddare, A. Salimi, Amplified fluorescent sensing of DNA using

luminescent carbon dots and AuNPs/GO as a sensing platform: a novel coupling of FRET and DNA hybridization for homogeneous HIV-1 gene detection at femtomolar level, Biosens. Bioelectron. 89 (2) (2017) 773-780.

[26] Y. Guo, Q. Chen, Y. Qi, Y. Xie, H. Qian, W. Yao, R. Pei, Label-free ratiometric DNA detection using two kinds of interaction-responsive emission dyes, Biosens. Bioelectron. 87 (2017) 320-324.

[27] Q. Guo, Y. Chen, Z. Song, L. Guo, F. Fu, G. Chen, Label-free and enzyme-free sensitive fluorescent detection of human immunodeficiency virus deoxyribonucleic acid based on hybridization chain reaction, Anal. Chim. Acta 852 (2014) 244-249.

[28] Q. Gong, Y. Wang, H. Yang, A sensitive impedimetric DNA biosensor for the determination of the HIV gene based on graphene-nafion composite film, Biosens. Bioelectron. 89 (1) (2017) 565-569.

[29] C. Jung, P. B. Allen, A. D. Ellington, A stochastic DNA walker that traverses a microparticle surface, Nat. Nanotechnol. 11 (2016) 157-163.

[30] X. Xiang, M. Luo, L. Shi, X. Ji, Z. He, Droplet-based microscale colorimetric biosensor for multiplexed DNA analysis via a graphene nanoprobe, Anal. Chim. Acta 751 (2012) 155-160.

[31] Q. Zhu, D. Xiang, C. Zhang, X. Ji, Z. He, Multicolour probes for sequence-specific DNA detection based on graphene oxide, Analyst 138 (18) (2013) 5194-5196.

[32] F. Li, J. Chao, Z. Li, S. Xing, S. Su, X. Li, S. Song, X. Zuo, C. Fan, B. Liu, W. Huang, L. Wang, L. Wang, Graphene oxide-assisted nucleic acids assays using

conjugated polyelectrolytes-based fluorescent signal transduction, Anal. Chem, 87 (2015) 3877-3883.

[33] J.Yan, H. Ma, P. Cai, J. Wu, Highly selective and sensitive nucleic acid detection based on polysaccharide-functionalized silver nanoparticles, Spectrochim. Acta. A Mol. Biomol. Spectrosc. 134 (2015) 17-21.

[34] J. Chen, Y. Liu, T. Ye, X. Xiang, X. Ji, Z. He, A novel droplet dosing strategy-based versatile microscale biosensor for detection of DNA, protein and ion, Sens. Actuators, B 215 (2015) 206-214.

[35] Y. Zhang, C. Zhu, L. Zhang, C. Tan, J. Yang, B. Chen, L. Wang, H. Zhang, DNA-templated silver nanoclusters for multiplexed fluorescent DNA detection, Small 11 (2015) 1385-1389.

[36] J. Chen, G. Zhou, Y. Liu, T. Ye, X. Xiang, X. Ji, Z. He, Assembly-line manipulation of droplets in microfluidic platform for fluorescence encoding and simultaneous multiplexed DNA detection, Talanta 134 (2015) 271-277.

[37] Q. Su, D. Xing, X. Zhou, Magnetic beads based rolling circle amplification-lectrochemiluminescence assay for highly sensitive detection of point mutation, Biosens. Bioelectron. 25 (7) (2010) 1615-1621.

[38] S. Laschi, R. Miranda-Castro, E. Gonzalez-Fernandez, I. Palchetti, F. Reymond, J. S. Rossier, G. Marrazza, A new gravity-driven microfluidic-based electrochemical assay coupled to magnetic beads for nucleic acid detection, Electrophoresis 31 (2010) 3727-3736.

[39] S. Wang, H. Yang, H. Zhang, F. Yang, M. Zhou, C. Jia, Y. Lan, Y. Ma, L. Zhou, S.

Tian, S. Wang, H. Zhang, Z. Chen, A surface plasmon resonance-based system to genotype human papillomavirus, Cancer Genet. Cytogenet. 200 (2) (2010) 100-105.

[40] J. Wang, Y. Wei, X. Hu, Y. Y. Fang, X. Li, J. Liu, S. Wang, Q. Yuan, Protein activity regulation: inhibition by closed-loop aptamer-based structures and restoration by Near-IR stimulation, J. Am. Chem. Soc 137 (33) (2015) 10576-10584.

[41] C. Chen, Y. Liu, Z. Zheng, G. Zhou, X. Ji, H. Wang, Z. He, A new colorimetric platform for ultrasensitive detection of protein and cancer cells based on the assembly of nucleic acids and proteins. Anal. Chim. Acta 880 (2015) 1-7.

[42] S. Lin, K. Chen, R. Liang, Thermal micro ATR/FT-IR spectroscopic system for quantitative study of the molecular structure of Poly (N-isopropylacrylamide) in water, Polymer 40 (1999) 2619–2624.

[43] Z. Zhao, Z. Li, Q. Xia, H. Xi, Y. Lin, Fast synthesis of temperature-sensitive PNIPAAm hydrogels by microwave irradiation, Eur. Polym. J. 44 (4) (2008) 1217-1224.

[44] Y. You, C. Hong, W. Wang, W. Lu, C. Pan, Preparation and characterization of thermally responsive and biodegradable block copolymer comprised of PNIPAAM and PLA by combination of ROP and RAFT methods, Macromolecules 37 (2004) 9761-9767.

Table 1. Capture capability of PNIPAAm-co-SA in buffer solution and serum.

Table 2. Recovery results of VV-targets in real human serum samples.

Table 3. Comparison of different methods for DNA detection.

Figure 1. Schematic illustration of principle for the preparation of PNIPAAm-co-SA.

Figure 2. (A) The FT-IR spectra and (B) DSC thermogram of PNIPAAm-co-SA. (C) UV−vis spectra for the thermal precipitation process of PNIPAAm-co-SA. (D) Fluorescence response for the specificity analysis with (a) PNIPAAm-co-SA + BF-DNA, (b) PNIPAAm-co-SA + F-DNA, (c) PNIPAAm + BF-DNA, (d) PNIPAAm + F-DNA. Experimental conditions: PNIPAAm-co-SA, 50 μL; PNIPAAm, 50 μL; BF-DNA, 6 nM; F-DNA, 6 nM.

Figure 3. The fluorescence intensities of different concentrations of BF-DNA. Experimental conditions: PNIPAAm-co-SA, 50 μL; BF-DNA, 12 nM, 20 nM, 40 nM, 100 nM, 200 nM, 400 nM.

Figure 4. Comparison of the capture capability in buffer solution and serum. Experimental conditions: PNIPAAm-co-SA, 50 μL; BF-DNA, 0.50 nM, 1.00 nM, 3.00 nM, 4.00 nM, 6.00 nM, 7.00 nM.

Figure 5. The investigation of the nonspecific adsorption. (a) PNIPAAm-co-SA + BF-DNA in PBS buffer solution. (b) PNIPAAm-co-SA + F-DNA in PBS buffer solution. (c) PNIPAAm-co-SA + BF-DNA in serum. (d) PNIPAAm-co-SA + F-DNA in serum. Experimental conditions: PNIPAAm-co-SA, 50 μL; BF-DNA, 6 nM; F-DNA, 6 nM.

Figure 6. The investigation of the storage life of PNIPAAm-co-SA. (a) newly-synthesized PNIPAAm-co-SA + BF-DNA. (b) stored for 45 days at 4°C PNIPAAm-co-SA + BF-DNA. Experimental conditions: PNIPAAm-co-SA, 50 μL; BF-DNA, 6 nM.

Figure 7. (A) Schematic illustration of principle for the sensitive detection of DNA. (B) The fluorescence responses at different concentrations of the target DNA: 0.50, 5.00, 10.00, 15.00, 20.00 nM (from bottom to top). Inset: the linear relationship between the fluorescence and the concentration of the target DNA. Experimental conditions: PNIPAAm-co-SA, 60 μL; Biotin-VV, 80 nM; VV-ROX, 80 nM.

Figure 8. The fluorescence responses in the presence of target DNA, two-base mismatched target DNA (MT2), three mismatched target DNA (MT3), four mismatched target DNA (MT4) and five mismatched target DNA (MT5), respectively. Experimental conditions: PNIPAAm-co-SA, 60 μL; Biotin-VV, 80 nM; VV-ROX, 80 nM; target DNA, 10 nM; MT2, 10 nM; MT3, 10 nM; MT4, 10 nM; MT5, 10 nM.

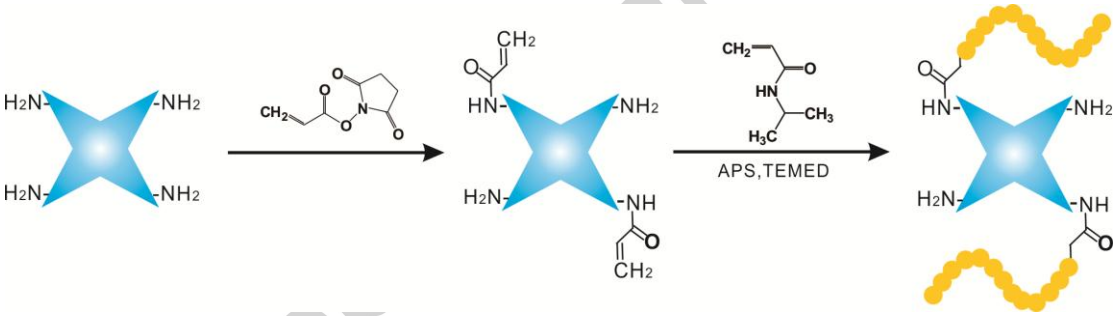

Fig. 1

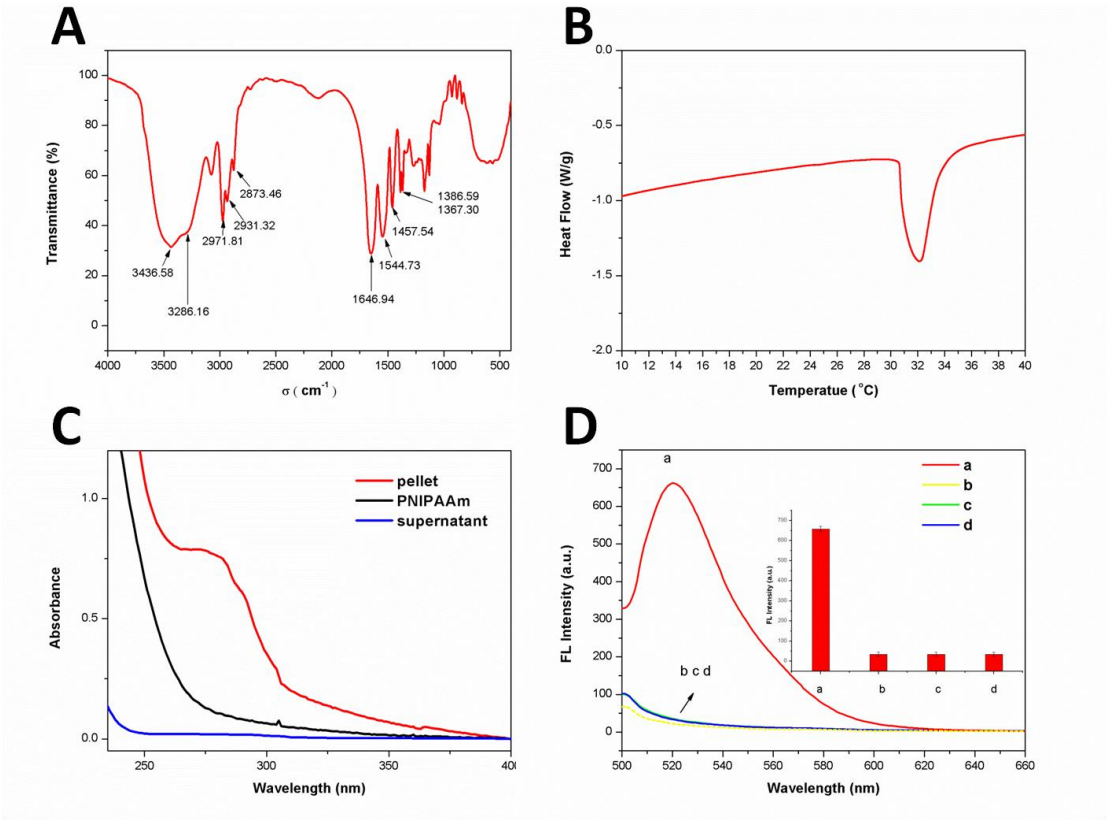
A
Transmittance (%)
σ (cm-1)
3436.58
3286.16
2971.81
2931.32
2873.46
1646.94
1544.73
1457.54
1386.59
1367.30
B
Heat Flow (W/g)
Temperatue (°C)
C
Absorbance
Wavelength (nm)
pellet
PNIPAAm
supernatant
D
FL Intensity (a.u.)
Wavelength (nm)
a
b
c
d
b c d

Fig. 2

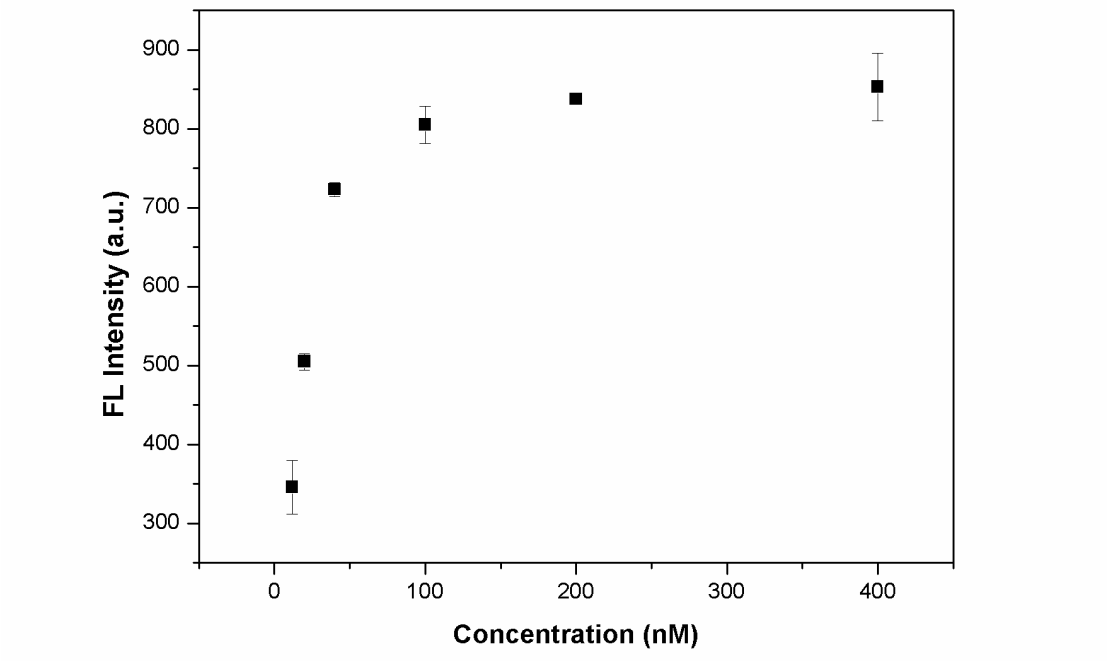
FL Intensity (a.u.)
Concentration (nM)

Fig. 3

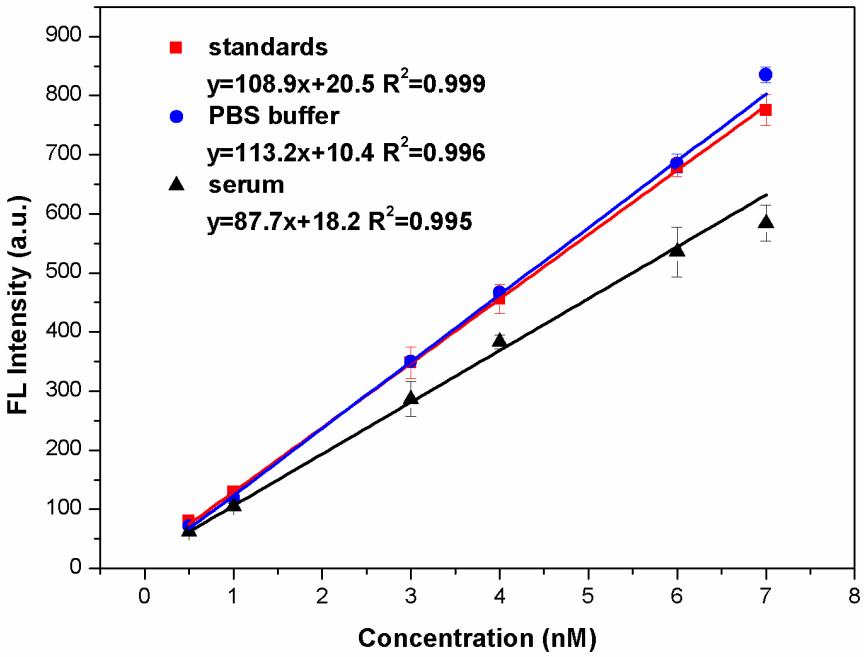
standards
y=108.9x+20.5 R2=0.999
PBS buffer
y=113.2x+10.4 R2=0.996
serum
y=87.7x+18.2 R2=0.995
FL Intensity (a.u.)
Concentration (nM)
0
100
200
300
400
500
600
700
800
900
0
1
2
3
4
5
6
7
8

Fig. 4

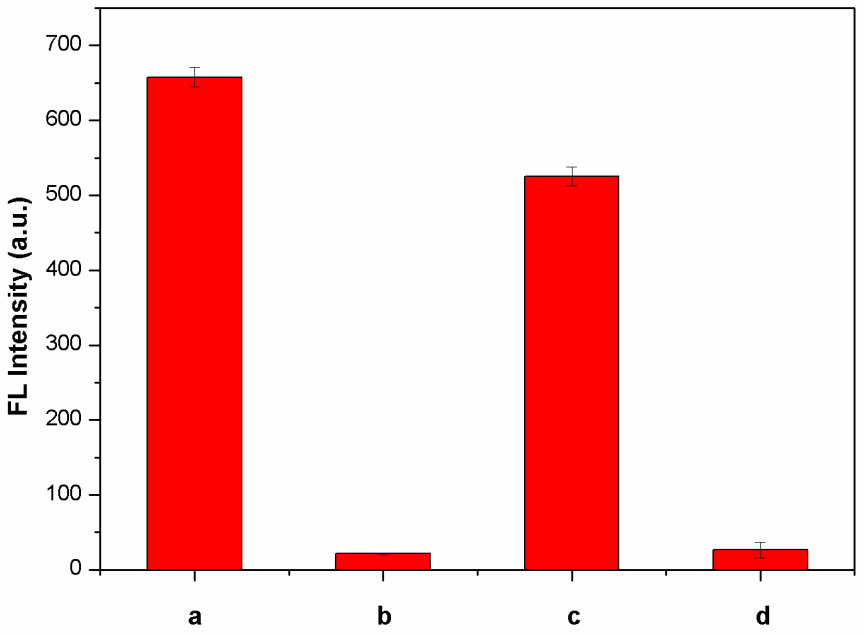
FL Intensity (a.u.)
0
100
200
300
400
500
600
700
a
b
c
d

Fig. 5

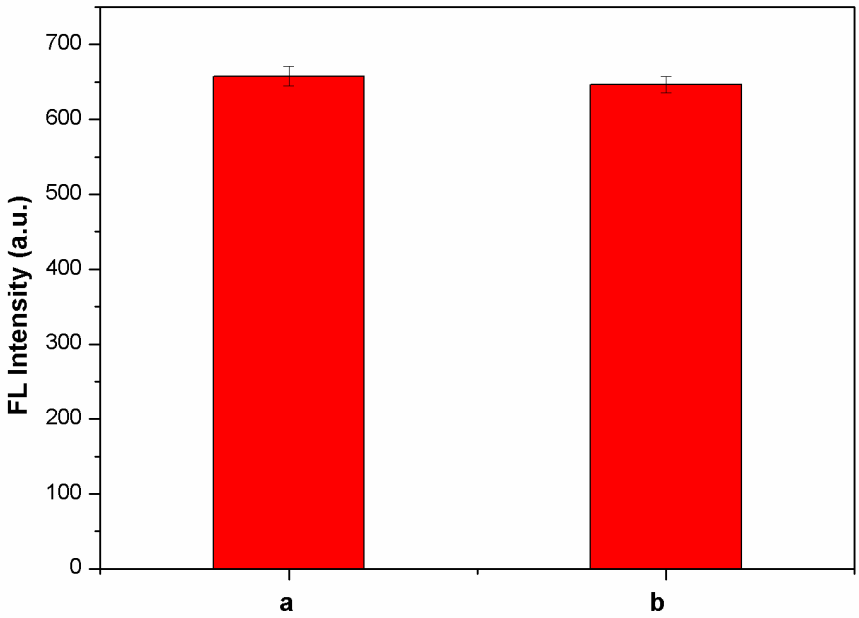

Fig. 6

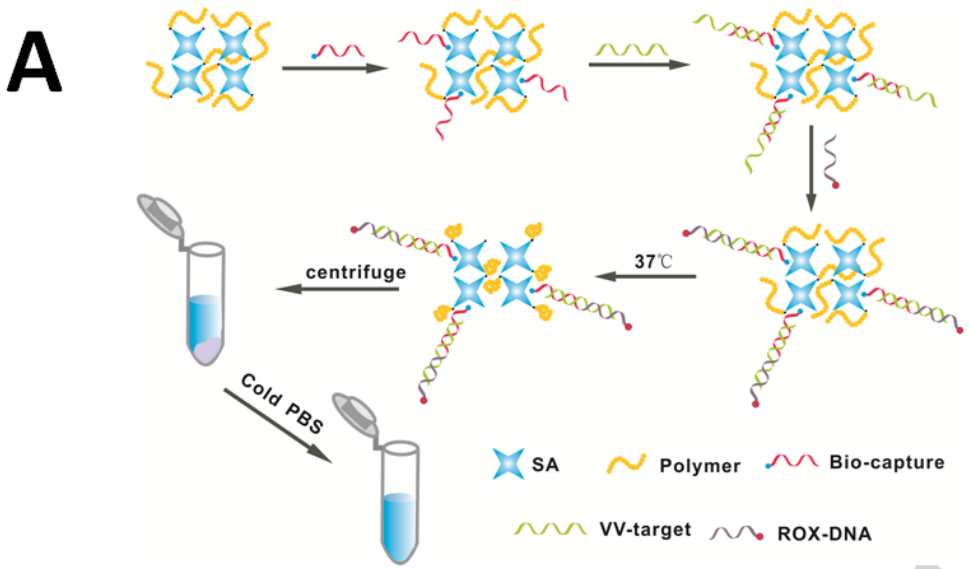
A
centrifuge
37℃
Cold PBS
SA
Polymer
Bio-capture
VV-target
ROX-DNA

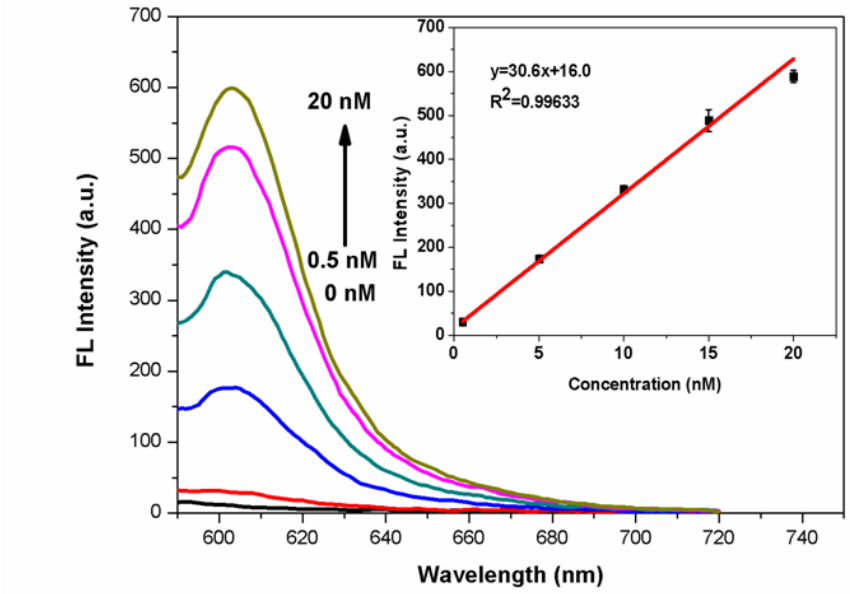
B
FL Intensity (a.u.)
Wavelength (nm)
20 nM
0.5 nM
0 nM
y=30.6x+16.0
R2=0.99633
Concentration (nM)

Fig. 7

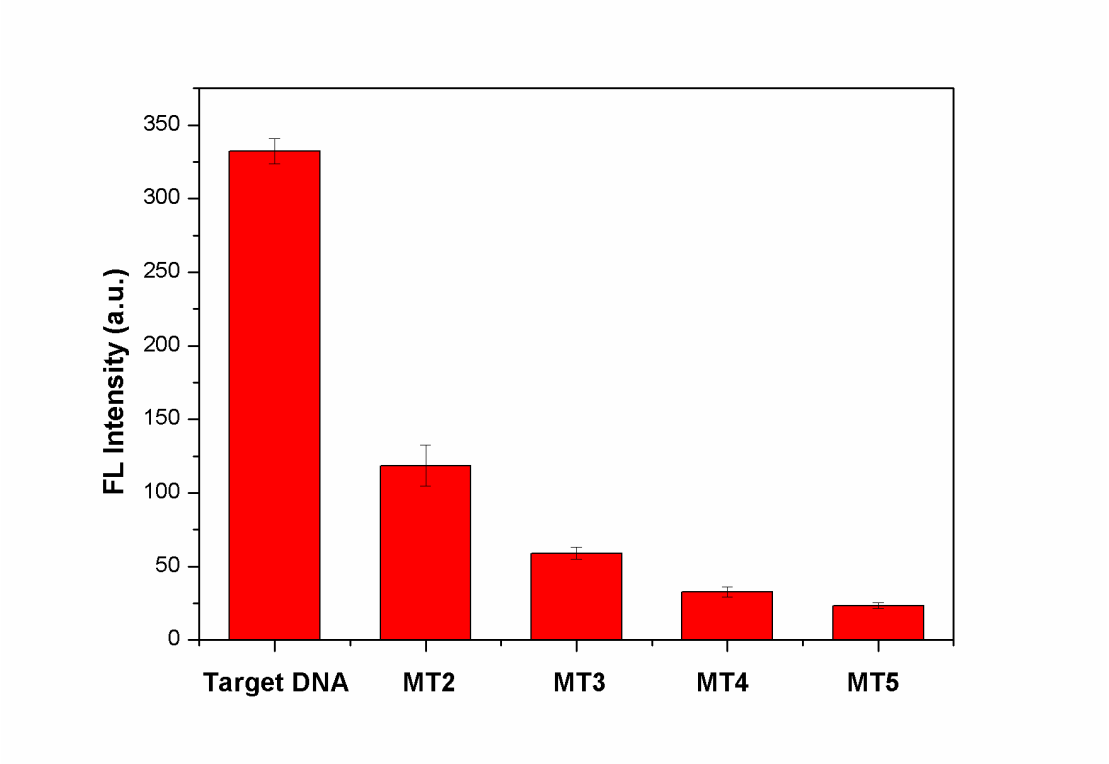

Fig. 8

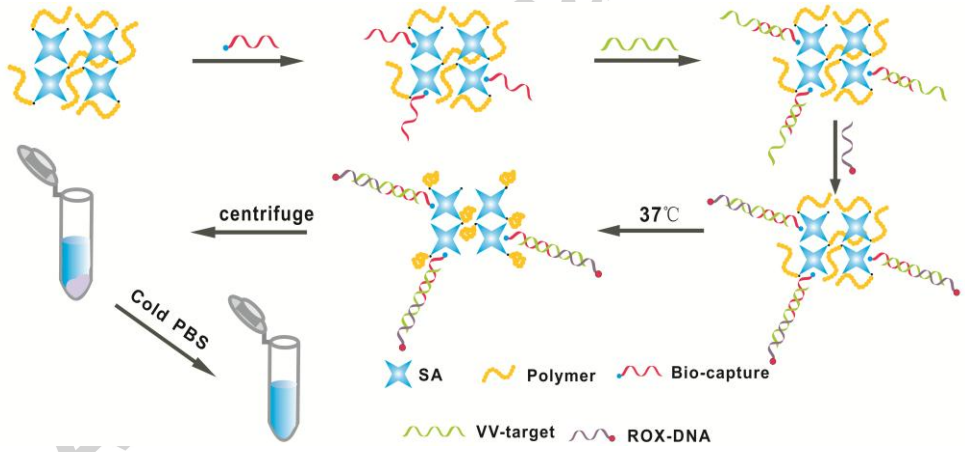

Graphical Abstract

Table 1. Capture capability of PNIPAAm-co-SA in buffer solution and serum.

Concentration (nM)	Capture rate (%)-PBS buffer solution	Capture rate (%)-serum
0.50	94	76
1.00	90.9	77.3
3.00	101	81.4
4.00	102	83.3
6.00	102	78.8
7.00	107	74.0

Table 2. Recovery results of VV-targets in real human serum samples.

Sample	Added (nM)	Found (nM)	Recovery (%)
1	5.00	5.58 ± 0.37	112
2	10.00	10.60 ± 0.81	106.1
3	15.00	15.54 ± 0.19	103.6
4	20.00	17.96 ± 0.21	89.80

Table 3. Comparison of different methods for DNA detection.

Detection method	Linear range	Detection limit	Ref.
Fluorescence detection	0.5-140 nM	0.29 nM	[26]
Fluorescence detection	3-30 nM	0.5 nM	[27]
Flow cytometry	not mentioned	5 nM	[29]
Colorimetric assay	0.1-10 μM	95 nM	[30]
Fluorescence detection	0.05-20 nM	50 pM	[32]
Fluorescence detection	2.5-25 nM	1.8 nM	[33]
Fluorescence detection	0.1-2 μM	25 nM	[35]
Fluorescence detection	0.025-5 μM	14 nM	[36]
Electrochemical assay	0.5-5 nM	0.33 nM	[38]
This work	0.5-20 nM	57 pM	

HIGHLIGHTS

1. An promising and stable thermosensitive composite was prepared.

2. Homogeneous reaction and heterogeneous separation could be realized.

3. The biosensor fabricated with PNIPAAm-co-SA exhibited high sensitivity.

4. Broad applicability could be achieved through simple changes in the future.